J. Fluid Mech. (1985), *vol.* 154, *pp.* 287–301
Printed in Great Britain

Finger-interaction mechanisms in stratified Hele-Shaw flow

By GRÉTAR TRYGGVASON† AND HASSAN AREF
Division of Engineering, Brown University, Providence, Rhode Island 02912

(Received 25 June 1984)

Interactions between a few fingers in sharply stratified Hele-Shaw flow are investigated by numerical integration of the initial-value problem. It is shown that fingers evolving from an initial perturbation of an unstable interface consisting of a *single* wave are rather insensitive to variations of the control parameters governing the flow. Initial perturbations with at least *two* waves, on the other hand, lead to important finger-interaction and selection mechanisms at finite amplitude. On the basis of the results reported here many features of an earlier numerical study of the 'statistical-fingering' regime can be rationalized.

1. Introduction

In their comprehensive review of multiphase flow through porous media Wooding & Morel-Seytoux (1976) discuss finger-selection, competition and interaction mechanisms in stratified Hele-Shaw flow. They comment that according to laboratory experiments on such flows the evolving interface morphology appears to depend sensitively on the viscosity ratio across the interface. On the other hand, since analytical studies of asymptotic, steady-state solutions to the so-called Hele-Shaw equations (Saffman & Taylor 1958; Saffman 1959) had not at that time revealed any such dependence, Wooding & Morel-Seytoux were led to speculate that the explanation of the laboratory observations involved three-dimensional effects not represented in the Hele-Shaw equations.‡

In an attempt to address these issues and others, we have developed a numerical implementation of the vortex-sheet approach to stratified Hele-Shaw flow with a sharp interface (de Josselin de Jong 1960), which allows simulation of solutions to the initial-value problem for flow regimes of relevance to reasonably large laboratory experiments (Tryggvason & Aref 1983, henceforth referred to as TA; see also Aref & Tryggvason 1984*a*). The studies reported in TA were primarily concerned with 'statistical fingering', i.e. with flows where many fingers of different shapes and sizes compete and interact. Initial conditions were chosen as 'random' collections of waves of different wavelengths and amplitudes. In this paper the emphasis is on more regular flows. Initial conditions with just one or two waves are considered, and the main objectives are to discover, characterize and quantify finger competition and interaction mechanisms as a function of a few available parameters in the initial state.

† Present address: Courant Institute of Mathematical Sciences, New York, NY 10012.

‡ We make a distinction between solutions to the Hele-Shaw equations and stratified flow in an actual Hele-Shaw cell. The degree to which the former represent the latter is a topic of ongoing debate and investigation. For recent work relating to one aspect of this, viz the pressure-jump condition at the interface, see Park & Homsy (1984) and Park, Gorell & Homsy (1984).

The main result that emerges is that single-wave initial conditions lead to essentially uniform arrays of similar fingers with little dependence on control parameters such as viscosity ratio or surface tension. However, even a slight admixture of a second wave in the initial state leads to finger competition and/or merging modes of evolution related to those seen for the statistical problems studied in TA.

We shall assume that the reader is familiar with or can refer to the general discussion in TA of basic equations, the vortex-sheet formulation and the description of numerical technique, and thus we shall concentrate here on presenting results. We simply repeat that there are two essential control parameters in the flow equations, viz the 'Atwood ratio' of viscosities A (viscosity difference over viscosity sum) and a non-dimensional surface-tension coefficient B.† Thus the objective of the present study is to discuss patterns of evolution from simple one- and two-wave initial conditions as a function of A and B. Accordingly, §2 is devoted to initial perturbations of a flat interface consisting of a single wave, whereas §3 explores the richer structure that ensues when the initial perturbation contains two waves. Our main conclusions are summarized in §4.

2. Single-wave initial conditions

In the past, studies of the finite-amplitude Taylor–Saffman instability have been concerned primarily with the asymptotic shape of a single finger propagating in a long, narrow Hele-Shaw cell (Saffman & Taylor 1958; Pitts 1980; McLean & Saffman 1981; Vanden-Broeck 1983). The motivation for these studies was the observation in laboratory experiments that, when a fluid of very small viscosity (typically air) drives out another of much larger viscosity (such as oil or glycerine), the final shape of the interface is usually a single, long, finger-shaped bubble. In the original paper by Saffman & Taylor (1958) on this subject, a family of asymptotic, steady-state solutions was found for the possible shapes of such a finger. These solutions assumed that surface-tension effects at the interface could be neglected ($B = 0$ in our notation, see §1 and TA) and left the ratio of finger width to channel width unspecified. This undetermined width ratio became the prime object of study in most investigations to appear over the following two decades. In recent years some measure of resolution has come about regarding this point. McLean & Saffman (1981) suggested that the inclusion of lateral surface-tension effects (i.e. those due to variations in the plane of the Hele-Shaw cell plates) determines the width ratio, and they produced steady-state profiles generated numerically to support this conclusion. However, subsequently Vanden-Broeck (1983) suggested that the solution found by McLean & Saffman was just one of a family of steady-state solutions, so that for any value of the (lateral) surface tension there would be a countably infinite number of possible fingers of different widths. No physical argument to support this 'quantization' of widths was given in Vanden-Broeck's brief study.

Since all these asymptotic fingers are steady states, which, furthermore, are believed to be unstable (McLean & Saffman 1981), it is essential to attempt to understand what role such flow patterns might play in an initial-value problem. In this connection it is of interest to recall an early solution obtained by Saffman (1959) that describes the temporal evolution of an interface perturbed initially by a

† Unfortunately equation (18) in TA defining B is slightly in error. The quantity B used in equation (16) of TA and elsewhere in that paper equals the right-hand side of TA (18) multiplied by $\frac{1}{2}$, i.e., in a gravity-driven cell of width W, $B = \alpha/(W^2 g\,\Delta\rho)$, where α is the surface-tension coefficient and $\Delta\rho$ the density drop at the interface, and g is the acceleration due to gravity.

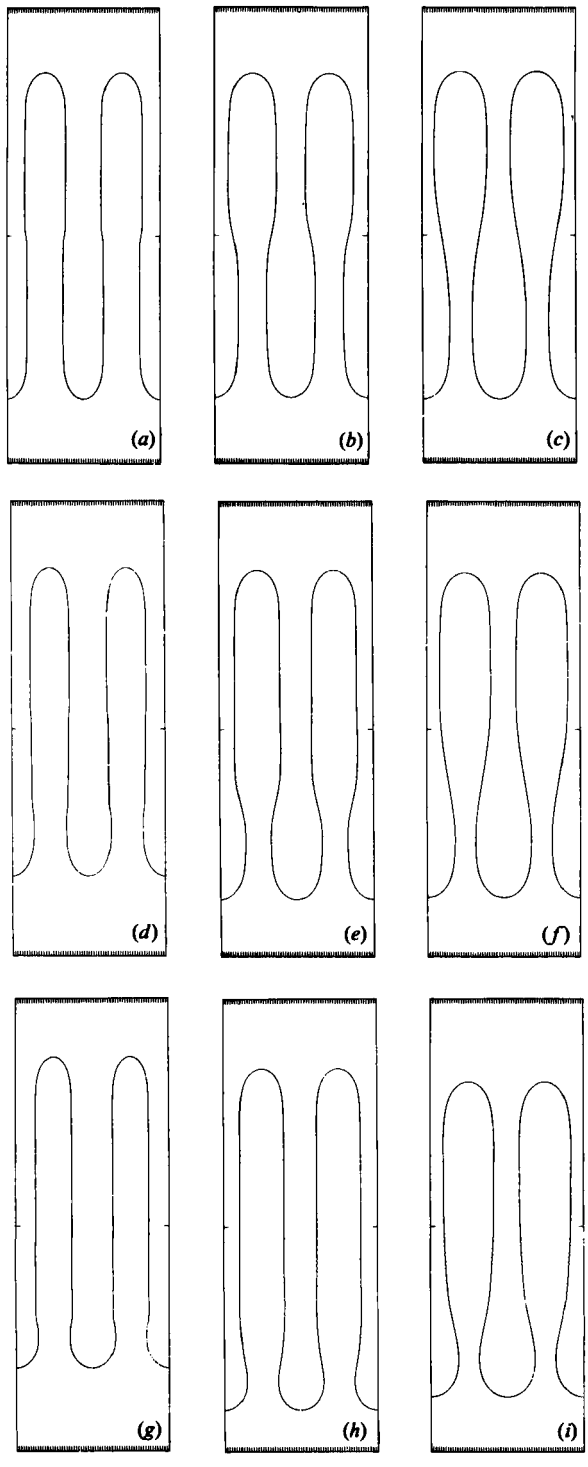

FIGURE 1. Nine finite-amplitude, identical-finger interfaces, resulting from single-wavelength perturbations of a flat interface at the position of the tickmarks on the long sides of individual frames. Values of control parameter A are 0 (a–c), 0.5 (d–f), 1 (g–i). Surface tension (parameter B) increases column by column from left to right, such that $\lambda_0/\lambda_f = 0.4$ (a, d, g), 1.0 (b, e, h), 1.67 (c, f, i).

small-amplitude sine wave. (This solution again neglects surface-tension effects, but assumes periodic boundary conditions in the direction along the interface.) In Saffman's (1959) solution, fingers of the more viscous fluid penetrate just as easily into the less viscous fluid as the converse, so that from the geometrical configuration of the interface at any instant one cannot tell which fluid is of greater viscosity. In general it is found both in numerical and laboratory experiments that the large-amplitude evolution is not up–down symmetric in this way, and thus the significance of this particular unsteady solution is unclear, as in fact already pointed out by Saffman (1959) (see also the remarks by Wooding & Morel-Seytoux 1976).

In this section we establish connections with these earlier investigations by computing the temporal evolution of an unstable interface, initially perturbed by a single (sine) wave of small amplitude, for various values of A and B. Figure 1 presents 9 large-amplitude shapes of interfaces produced in this way. The initial mean position of the interface is given by the tickmarks on the long side of individual frames. It was argued and checked in TA that for an interface perturbed by an assembly of waves the relevant lengthscale is the length of the most unstable wave (λ_0, say) which is determined by surface tension (i.e. the value of B). When the interface is perturbed by a single wave of a specific wavelength λ_f (as done in figure 1) that is, of course, no longer true. Now the wavelength imposed is of importance and the effect of surface tension (parameter B) is described by a ratio λ_0/λ_f of the most unstable wavelength to the imposed wavelength. The results in figure 1 show interfaces for which λ_0/λ_f is less than one (figures 1*a*, *d*, *g*; $\lambda_0/\lambda_f = 0.4$), equal to one (figure 1*b*, *e*, *h*) and greater than one (figures 1*c*,*f*, *i*; $\lambda_0/\lambda_f = 1.67$). Actually this last set of results corresponds to such a large value of B that λ_f is almost within the domain of linearly stable waves.† By using an initial perturbation of sufficiently large amplitude, however, the interface can usually be 'pushed' beyond the linearly stable regime. Analytical studies of steady states frequently report on high-surface-tension regimes wherein the interface is actually linearly stable.

For the particular numerical scheme we are using, low-surface-tension cases (small B) require that the numerical resolution is sufficiently high so that disturbances that are stabilized by surface tension are on the scale of a grid spacing or smaller (see TA).‡ Our computational domain is periodic in the direction along the interface, and we have chosen to show two periods for each case, although in some cases only one period was actually computed. We found that for small A and small B (upper left in figure 1) our code would faithfully simulate two periods retaining the periodicity exactly. For large A and large B (lower right in figure 1), on the other hand, numerical disturbances could amplify and lead to loss of periodicity at the largest amplitudes. Physical mechanisms responsible for such behaviour will become clear in §3. In a couple of instances lopsided, asymmetrical fingers emerged, apparently triggered by some asymmetry in the redistribution of computational points. Asymmetric fingering was discussed briefly by Birkhoff (see Taylor & Saffman 1958) and by Taylor & Saffman (1959), but seems not to have received further study.

For a fixed value of A figure 1 shows that the width of the evolving fingers increases with increasing surface tension, in qualitative agreement with the steady-state results of McLean & Saffman (1981). (Quantitative aspects of this are discussed below.) For small surface tension (small B, figure 1*a*, *d*, *g*) differences between the finger patterns

† The linearly stable regime starts at $\lambda_0/\lambda_f = \sqrt{3}$.

‡ In figures 1, 3, 5 and 7 the resolution of the Eulerian grid is apparent from the tickmarks at one end of individual frames.

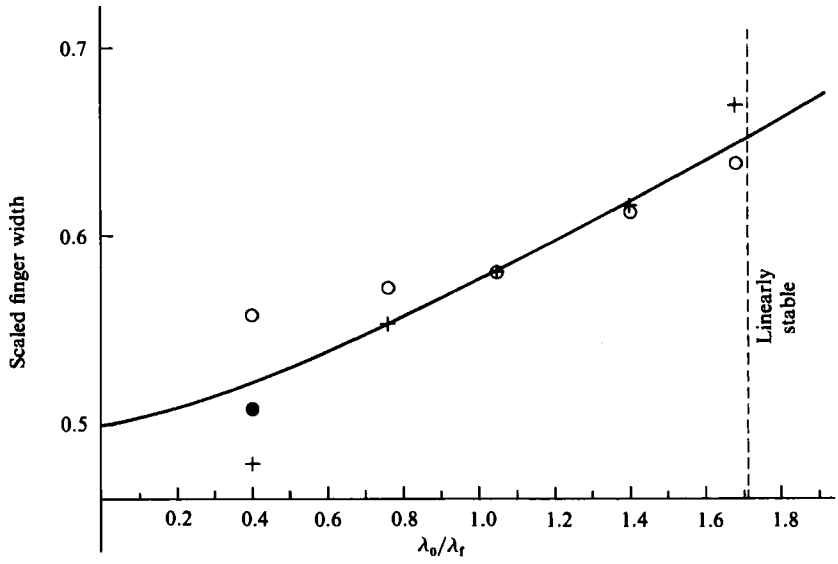

FIGURE 2. Comparison of computed, asymptotic finger widths (per unit width of computational domain) to corresponding steady-state results of McLean & Saffman (1981) (solid curve) as a function of λ_0/λ_f. Symbols correspond to different spatial resolutions as follows: +, 32; ●, 16; ○, 8 grid spacings per finger.

for different values of A are slight, as one might expect on the basis of Saffman's (1959) solution. For larger values of B a surface-tension-dependent 'drop' appears in the finger pattern (figure 1 *c*, *f*, *i*). The position and size of this additional 'drop' depends on A. For $A = 0$ the interface must evolve in an up–down symmetric way (see TA) and the fingers expand at the position of the initial interface (figure 1 *a*–*c*). For non-zero A non-symmetrical patterns result (figure 1 *e*, *f*, *h*, *i*).

For $A = 1$ we have compared our evolving fingers quantitatively to the steady-state solutions obtained by McLean & Saffman in two ways. First, in figure 2 we have plotted the maximum width (per unit width of the computational domain) of the finger of 'inviscid' fluid† versus λ_0/λ_f for the $A = 1$ runs in figure 1 and for two additional runs (with $\lambda_0/\lambda_f = 0.75$ and 1.4 respectively). Our data points (crosses, other symbols are explained below) are shown superimposed on the graph obtained by McLean & Saffman for steady states.‡ It is seen that particularly good agreement between long-time evolution and steady-state results is obtained for values of $\lambda_0/\lambda_f \approx 1$. For small and large values of this ratio deviations appear in our asymptotic, scaled widths. In both limits we are presumably seeing effects of imposing on the evolving interface a perturbation wavelength that is well removed from the dynamically most unstable mode. For $\lambda_0/\lambda_f = 1.67$ we believe that the deviation of our points from the curve in figure 2 is due to incomplete relaxation and equilibration of the finger. As mentioned previously, λ_f is here almost in the linearly stable regime, and it was necessary to start the calculation with a sizeable amplitude of the perturbing wave, considerably larger than that used for the runs that make up the middle column in figure 1. Because of the mismatch between preferred and imposed

† As mentioned in TA, the limit $A = 1$ is slightly artificial. The 'inviscid' fluid is still assumed to satisfy the (limiting form of the) Hele-Shaw equations and not Euler's equation.

‡ Our figure 2 is equivalent to figure 4 of McLean & Saffman (1981). We are indebted to Dr McLean for sending us several tables of data relating to his computed steady-state solutions.

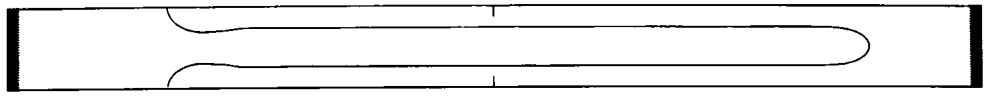

FIGURE 3. Very-large-amplitude finger for $A = 1$, $\lambda_0/\lambda_f = 0.4$. The underlying grid is 32×384. This finger appears highly regular and stable. It is some 8% thinner than the corresponding McLean & Saffman (1981) steady state.

spatial periodicity the equations of motion become somewhat stiff in this case and the computations leading to figure 1 (*i*), in particular, were more demanding of resources than one might expect.

The situation for $\lambda_0/\lambda_f = 0.4$ is more difficult. The fingers that we produce are some 8% narrower than the corresponding McLean & Saffman steady state. As shown in figure 3, we have run this particular finger to more than twice the amplitude shown in figure 1 (*g*) in the hope that it would widen somewhat as the relaxation progressed. (We argue at the end of §3.1 that for $\lambda_f > \lambda_0$ fingers will approach their asymptotic width from below.) This did not happen. We have varied the interplay between time-stepping and point-redistribution algorithms (cf. TA) in various ways in the hope of discovering purely numerical reasons for the thin fingers. Again we could produce no change. Finally we have considered the effect of grid resolution on all runs. As figure 1 shows, the resolution used is such that each finger spans 32 grid spacings. On a coarser grid, e.g. one with only 8 grid spacings over the width of a finger, one may expect grid effects to act as an artificial surface tension and thus fatten fingers. (This is not rigorously true, e.g. the dispersion relation in linearized theory is different; cf. TA.) This behaviour is indeed observed (see the open dots in figure 2) for low λ_0/λ_f. For larger values of λ_0/λ_f grid effects are slight even after coarsening the grid by a factor of 4 (this feature is discussed again when we come to figure 4). For $\lambda_0/\lambda_f = 0.4$ we also show the asymptotic width for a resolution of 16 grid spacings per finger (solid dot). The results in figure 2 suggest that we do achieve convergence under grid refinement, but for $\lambda_0/\lambda_f = 0.4$ this convergence is unmistakably towards a finger pattern with narrower fingers than any of the known steady-state solutions (with surface tension). We have no conclusive explanation for this result. It may point to a shortcoming of our numerical procedure in this limit, or it may indicate some as yet undiscovered bifurcation phenomenon. In any case we shall not pursue this issue further here, since we shall obtain a better understanding of the significance of single fingers for interface evolution later. We should, however, emphasize that, since the calculations reported in TA were for freely evolving interfaces, they always corresponded to the regime of figure 1 (*b*, *e*, *h*), at least during early stages.

As a second more detailed check on our methodology we have compared the full single-finger profile of figure 1 (*h*) with the appropriate steady-state finger of McLean & Saffman (1981), again using data kindly provided by Dr McLean. Figure 4 summarizes the results of this comparison. The solid curve gives data from the McLean & Saffman calculations of steady-state profiles. It consists of two parts: a detailed 'nose' profile and an asymptotic width. Both parts are shown in figure 4. Also shown are the positions of vortex elements representing the interface in our computational scheme (see TA) for two different runs. The crosses represent Lagrangian vortex elements on the finger (after considerable evolution) using an underlying Eulerian grid (see TA) with a resolution as indicated by the tickmarks at the extreme left of figure 4 (32 grid spacings per finger). The agreement is obviously excellent. The open dots provide similar data for a run where the Eulerian grid was

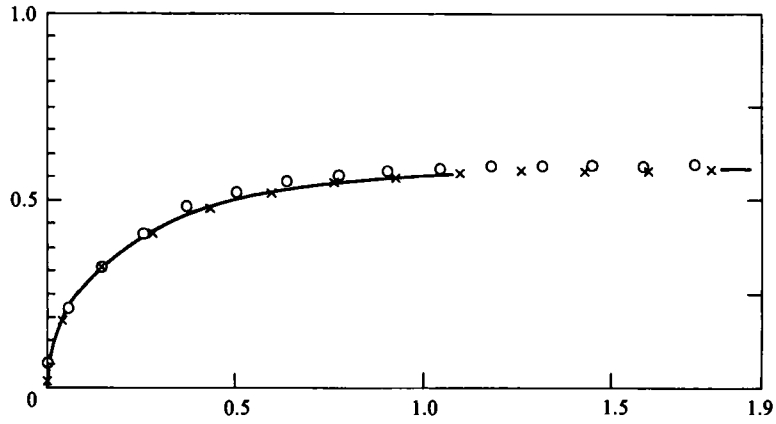

FIGURE 4. Comparison of computed, asymptotic finger profile for $A = 1$, $\lambda_0/\lambda_f = 1$, to steady-state solution of McLean & Saffman (1981) (solid curve). Symbols indicate instantaneous positions of some vortex elements, and correspond to different spatial resolutions as follows: ×, 32 grid spacings per finger (tickmarks at left), ○, 8 grid spacings per finger (tickmarks at right).

four times coarser, with a resolution indicated by the tickmarks at the extreme right of figure 4 (8 grid spacings per finger). We see that the agreement is still very satisfactory, in spite of the substantial nominal decrease in Eulerian resolution (resulting, incidentally, in a considerably reduced demand on computer resources). We note that not all the vortex elements actually used in the computations are shown in figure 4. It thus appears that our hybrid Eulerian–Lagrangian code (see TA) retains a remarkable degree of spatial 'subgrid' resolution. Well-known sources of numerical error such as grid-induced velocity anisotropy (cf. Aref & Siggia 1980) are not in evidence. This is all very encouraging for applications to statistical flow regimes. However, we must mention (as already remarked in TA) that the evolution *in time* on the coarser grid is somewhat slower than on the fine grid.

We conclude this section with miscellaneous remarks and comments. (i) The calculations reported in TA used spatial resolutions per interfacial structure intermediate between the two cases illustrated in figure 4. (ii) The relaxation to asymptotic steady states of the type found by McLean & Saffman in our initial-value calculations makes the currently predicted linearized instability of these states seem even more paradoxical. It has always been possible to rationalize the emergence of single fingers in experiments by appealing to stabilizing physical mechanisms conceivably present in the experimental setup but definitely absent from the Hele-Shaw equations. Our calculations strongly suggest the emergence of steady-state fingers entirely within the framework of the Hele-Shaw equations. When 'grown' from single-wavelength initial perturbations these fingers appear very stable.† (iii) Although the agreement between our numerical results and analytic theory seems quite satisfactory, the main virtue of a vortex-in-cell-based code is the reduction in operation count per time step. This feature allows such a code to probe statistical flow regimes. However, the introduction of an Eulerian grid allows a multitude of numerical artifacts to enter the calculations, including the anisotropy alluded to above. Also the spatial cutoff at small scales

† We are indebted to Professor L. P. Kadanoff, Dr B. Shraiman and Dr D. Bensimon for an interesting discussion in which this point was emphasized. The same point was raised by Professor P. G. Saffman following the presentation in Aref & Tryggvason (1984*b*).

imposed by the grid essentially dictates use of a surface tension at the interface. For these reasons, and in view of the potential problems mentioned above for small surface tension, we do not advocate use of this type of code for probing sensitive analytical issues (e.g. singularities after a finite time for vanishing surface tension) involving initial conditions with just one or two wavelengths. For such investigations direct summation implementations of the boundary integral method† are practicable and probably preferable. (iv) As far as we are aware, we have not seen any manifestations of the spectrum of auxiliary steady-state solutions proposed by Vanden-Broeck (1983). This comment is not intended to question his analysis, but simply to record that we have no idea at present on how to generate such solutions in an initial-value calculation.

3. Two-wave initial conditions

In order to gain an understanding of the underlying physical mechanisms responsible for interfacial patterns in stratified Hele-Shaw flow, it is desirable to study solutions to the equations of motion that are simple yet capture essential elements of the interaction processes observed. The identical-finger solutions discussed in §2 obviously do capture the most fundamental aspect of an unstable interface, viz the appearance of fingers. However, just as obviously, such solutions give few hints as to the complex interactions that may occur between different fingers at large amplitudes. And one knows from laboratory experiments (e.g. Wooding 1969) that the long-time evolution of an interface is in general influenced by the outcome of such interactions. Specifically, the single-finger solutions of §2 showed considerable *insensitivity* to the control parameter A (see figure 1), which we know from TA exerts a profound influence on interface evolution in the statistical-fingering regime. One question that arises, then, is how many waves are required for the main modes of finger competition and finger merging observed in the statistical problem. As we shall see in this section initial conditions with just two waves can lead to several of the main interaction patterns observed previously in TA for evolution from 'random' initial conditions.

3.1. *Finger competition and selection*

Examples of evolution of two-wave initial conditions for $A = 0$, 0.5 and 1 (and fixed B) are shown in figure 5. The general amplitude of the main perturbing wave, of wavelength close to the most unstable wave, is clear from the first frame in each sequence, but there is actually an admixture of a second wave of twice the wavelength and 20% of the amplitude. During initial stages of evolution the interface shape is largely independent of A. (This is consistent with linearized stability analysis, where the growth rates of unstable waves are independent of A.) However, as the fingers grow the sequences in figure 5 differentiate themselves according to the value of A as the effect of the second wave becomes evident.

Comparing the results of this two-wave initial perturbation to the results of single-wave initial conditions from §2 (figure 1), we see that the amplitude retardation imparted to every other finger in figure 5 amplifies in time for all values of A, so that, instead of having two identical fingers in the final panels of figure 5, the middle finger

† Professor G. R. Baker informs us that he has recently completed such a code.

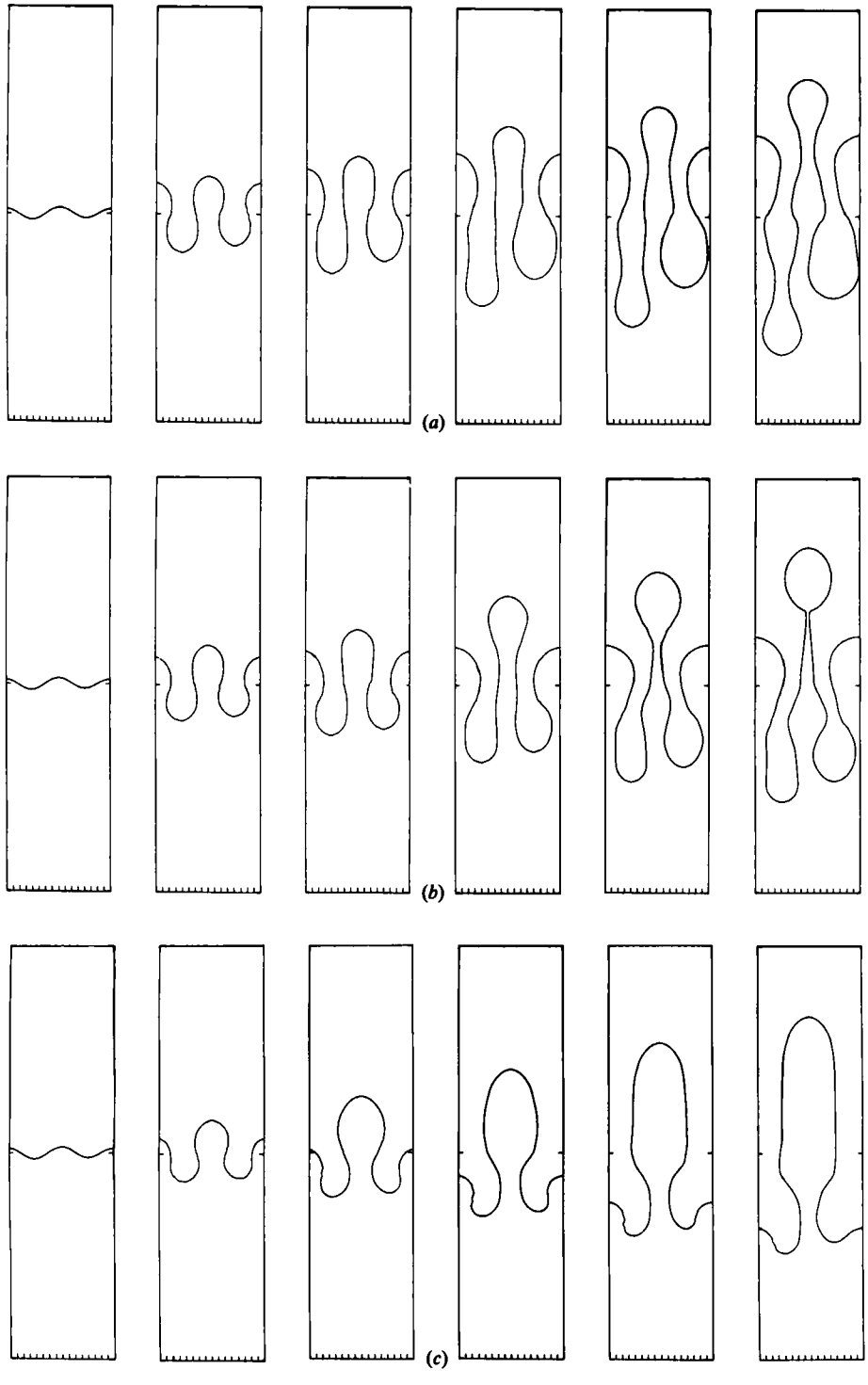

FIGURE 5. Three time sequences of evolving interfaces started from a perturbation of a flat interface consisting of a basic wave with a 20% admixture of a wave of twice the wavelength. For all runs $\lambda_0 \approx \lambda_f$ (for the basic wave) and (*a*) $A = 0$, (*b*) 0.5, (*c*) 1. Note the selection of the finger growing out of the highest crest of the initial perturbation.

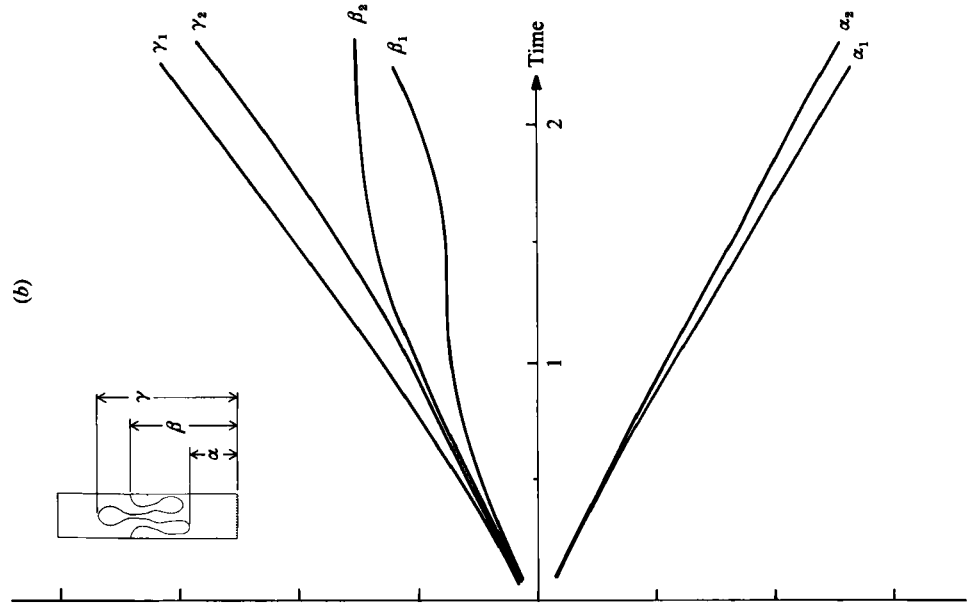
(b)
γ_1
γ_2
β_2
β_1
Time
2
1
α_2
α_1
γ
β
α

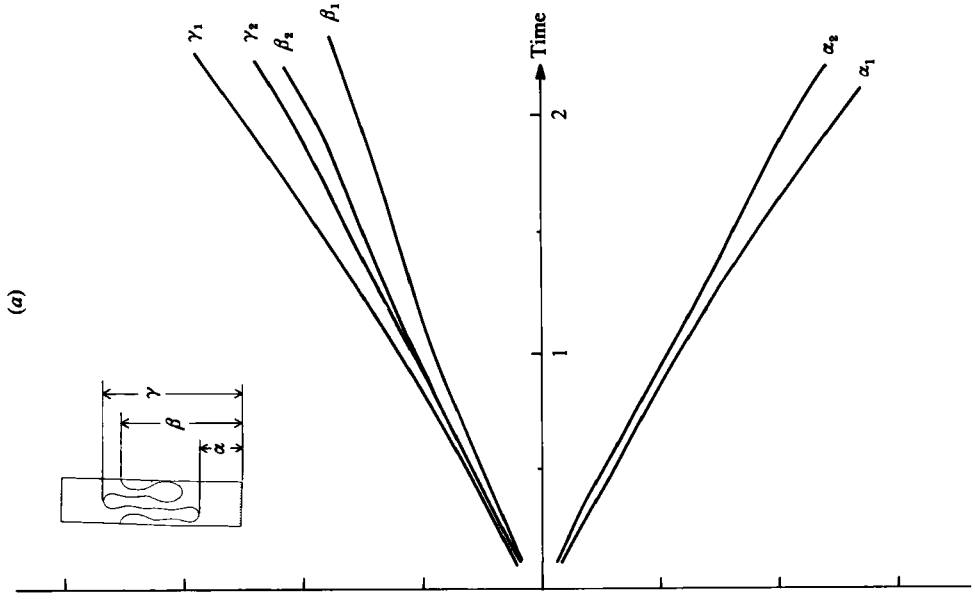
(a)
γ_1
γ_2
β_2
β_1
Time
2
1
α_2
α_1
γ
β
α

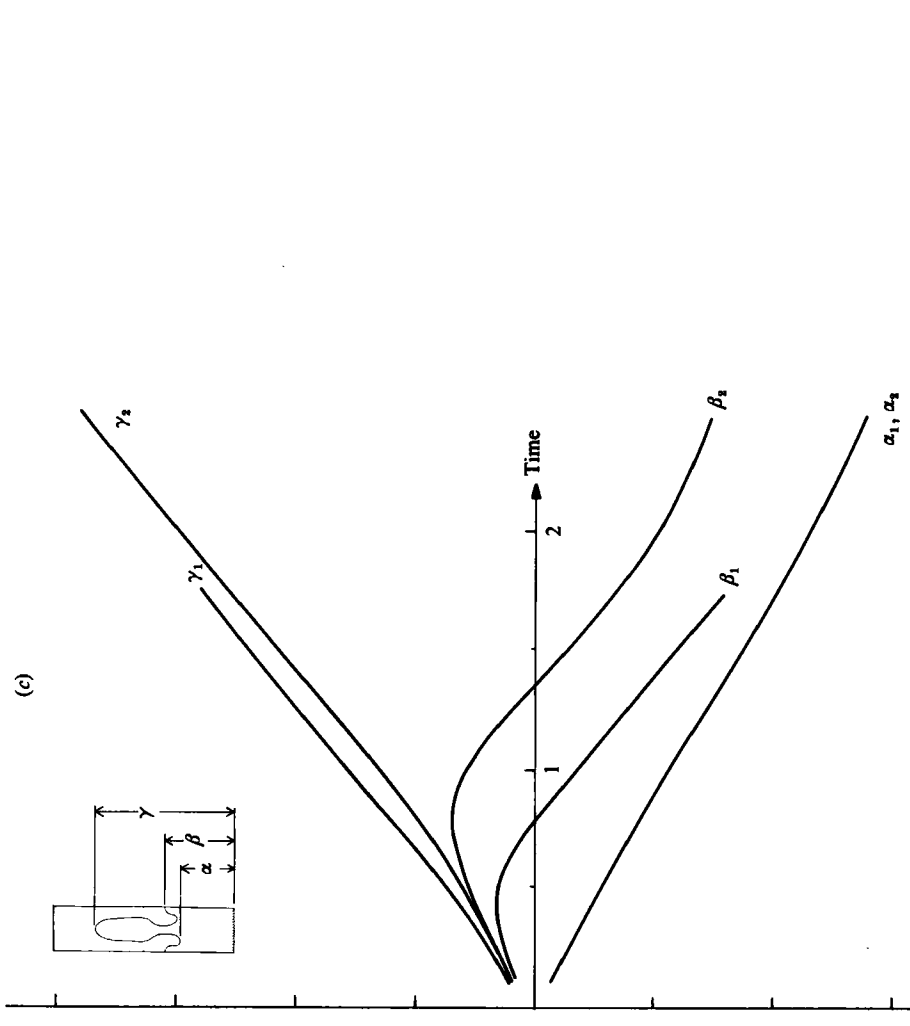

FIGURE 6. Heights of 'peaks' and 'valleys' as a function of time for the three runs in figure 5. The inset sketch shows the definition of α, β, γ. Subscript 1 corresponds to the runs shown in figure 5. Subscript 2 corresponds to similar runs in which the initial amplitude of the longer perturbing wave was only 2% of that of the basic wave. Units are of little significance, are the same for the three cases, and are included only to aid comparisons.

is longer than the finger straddling the periodic boundary. This selection mechanism increases in importance with increasing values of A.

The asymmetry between the degree of penetration of more viscous and less viscous fluid for non-zero A, which was so obvious in the statistical flows of TA, is thus seen to manifest itself already for two-wave initial perturbations. In this sense, then, the single- (or identical-) finger solutions of §2 must be considered rather special. Initial perturbations with more than a single wavelength (as one would generally expect in practice) will lead to competition and selection processes. Nevertheless, if for $A = 1$ one compares the tip of the surviving finger in figure 5(*c*) to a solution of the type shown in figure 1, it is found that the finger profiles are very close. Thus for $A = 1$ the asymptotic results for single-finger shapes do appear relevant in general (we return to this feature at the end of this subsection). However, for smaller values of A the asymptotic state of the largest finger evolving from a two-wave initial perturbation appears distinctly different from the single-wave fingers of §2.†

In an attempt to quantify these observations we have monitored heights of various 'peaks' and 'valleys' of the interface profile as a function of time. Figure 6 shows data of this type. Time is along the abscissa, and the heights defined in the inset sketch are plotted along the ordinate. Time histories corresponding to the interfaces shown in figure 5 carry a subscript 1. Another similar run with a second-wave amplitude of just 2% of the main-wave amplitude leads to growth of primary and secondary fingers given by the curves subscripted 2 in figure 6. Let us now comment on these graphs. First, for $A = 0$ the graphs γ_1, γ_2 follow immediately from α_1, α_2 by symmetry. For $A > 0$ this is no longer true, and the increasing up–down asymmetry that has been mentioned several times already is evident in figure 6 also. Secondly, as expected, the graphs β_2, γ_2 follow each other more closely than β_1, γ_1 because the initial amplitude of the second wave is ten times smaller. In the absence of a second-wave perturbation we would revert to the identical-fingering process of §2, and the β- and γ-graphs would coincide. The effect of A is seen to manifest itself in that β and γ separate much earlier and more decisively for large A (figure 6*c*) than for small A (figure 6*a*). In fact for $A = 1$ the secondary fingers can apparently be pulled down completely, and should be entirely eroded away with time, i.e. the β_1 graph bends over and tends towards the α_1 graph in figure 6(*c*). For $A = 0$ the secondary fingers continue to grow. For intermediate A, for example $A = 0.5$ (figure 6*b*), the ultimate fate of secondary fingers seems to depend on the magnitude of the initial perturbation.

A most interesting feature of figure 6 is that the growth of the total width of the finger region, i.e. $\gamma - \alpha$, is sensitive to the interactions going on within. For all A the strongly perturbed interface (case 1) grows somewhat faster than the weakly perturbed one (case 2). The ultimate growth rates (slopes of α_1, α_2 and γ_1, γ_2) are similar, but there is a 'delay' as if interactions between the fingers have to 'sort out' which fingers will 'lead' and which will 'follow'. For $A = 1$ the α-graph is completely insensitive to these amplitudes of second-wave perturbation, as one might expect.

We point out that the result obtained in figure 5(*c*) suggests that for $A = 1$ fingers with $\lambda_f > \lambda_0$ approach their asymptotic width from below. For suppose the calculation in figure 5(*c*) continued until essentially just one long, asymptotic finger remained.

† We have, of course, only shown a difference at finite amplitudes, but we find it difficult to see how the interface in figure 5(*b*) can relax to a finger of the type shown in figure 1(*e*). In fact the two-wave initial condition can probably lead to droplet pinch-off at the finger tip.

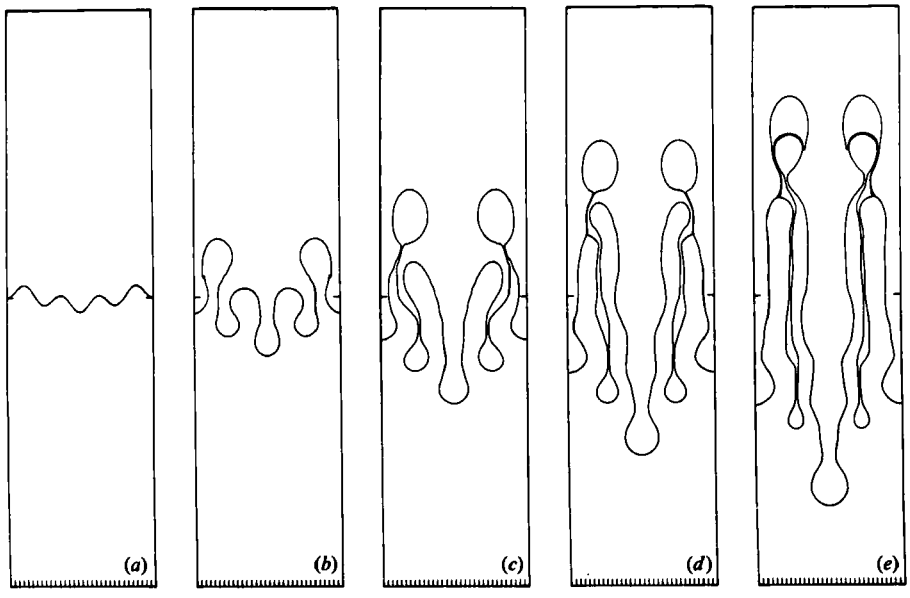

FIGURE 7. An example of finger merging and droplet pinch-off generated from a two-wave initial condition with perturbing waves of wavelength ratio 4:1. For this case $A = 0.5$, the two perturbing waves have the same amplitude, and the shorter wavelength is close to the most unstable wavelength λ_0.

Since this finger initially came from a wave with dominant wavelength close to λ_0, and since it is approaching twice the width one would expect for a pure single-wave initial condition with wavelength λ_0, it must correspond to the regime $\lambda_f > \lambda_0$ in the context of figure 1. Clearly in this specific evolutionary sequence the finger approaches its asymptotic width from below. This argument was the basis for the hope that the finger in figure 1 (*g*) would 'fatten' upon further evolution (see §2).

The results in figures 5 (*c*), 6 (*c*) also suggest that for $A = 1$ the surviving asymptotic finger corresponds to the longest excited wave of the initial state, even though this wave may only be present with a small amplitude. The longest wavelength available in a real Hele-Shaw cell equals the width of the cell.

3.2. *Finger merging*

If the wavelengths of the two perturbing waves have a ratio different from 2:1 other modes of finger interaction, in particular finger merging, become possible for $A < 1$. Consider, for example, the case shown in figure 7 where the two waves have wavelengths of ratio 4:1. In this example $A = 0.5$, and B was chosen such that the wavelength of the shortest perturbing wave is close to the linearly most unstable wave. The two perturbing waves are of the same amplitude as seen in the plot of initial condition (figure 7*a*). The relatively large amplitude of the longer perturbing wave was chosen so that the finger interactions of interest could take place at reasonably low overall amplitude. As we have seen in §3.1, the time delay for a second-wave perturbation to manifest itself increases with decreasing amplitude of the wave. This is also true for finger-merging modes.

We have not pursued in detail how aspects of finger merging depend on the waves present in the initial state. Our main point is that such modes are accessible already

from entirely regular two-wave initial conditions, and thus must be expected to occur quite generally. We have already commented in TA on the physically plausible way that our code handles dynamically inert double interfaces resulting from finger merging or droplet pinch-off.

4. Conclusions

By numerical calculations of the initial-value problem for a sharp interface evolving according to the Hele-Shaw equations we have shown the following.

(1) Single- (or identical-) finger solutions can be obtained for arbitrary values of A by considering initial perturbations with only a single wavelength. There are effects of surface tension to be seen in these solutions, and these are coupled to the value of A, but on the whole single-finger solutions are insensitive to this main control parameter. When the perturbation wavelength agrees with the linearly most unstable wavelength, the computed long-time finger for $A = 1$ agrees with asymptotic steady-state solutions of McLean & Saffman (1981).

(2) Even a slight admixture of a second wave leads to finite-time evolution patterns that can be very different from the identical-finger results. Impeding some fingers initially typically leads to their demise with time, and this finger-selection mechanism becomes stronger as A increases. The asymptotic shape of surviving fingers is similar to the identical-finger solutions for $A = 1$, but appears to deviate from this for $A < 1$.

(3) Finger collision, merging and droplet pinch-off can be achieved for $A < 1$ starting from two-wave initial perturbations.

It is tempting to conclude that all the results of the statistical-fingering calculations in TA could have been obtained using flows with just a few fingers (and thus much cheaper computations). Such a conclusion would be unfounded. On one hand we could not know *a priori* if, for example, three-finger collisions would be important, and the only way to check for this kind of collective effects is to simulate flows on such a scale that these effects have a chance to manifest themselves. On the other hand, there are details of the complex interfaces simulated in TA that defy the simpler calculations considered here. (The finger-splitting event observed for $A = 0.5$ (see figure 6 of TA) is an example.) Our main point is that with two-wave perturbations we can 'synthetically' produce, and hence make considerable headway towards understanding, some of the main finger interaction and competition mechanisms that one observes for statistical interfaces.

Since solutions with periodically repeated, identical fingers miss several essential dynamical processes for an evolving interface, the studies presented here illustrate, through a rather simple example, how misleading it can be to attempt to predict the finite-amplitude behaviour of fluid motions by analyses based on steady states and linearized stability considerations. Although steady states are valuable, because they are usually exact, mathematical solutions, initial-value calculations are essential in order to capture the full dynamical evolution.

We acknowledge support for this work by National Science Foundation grant MEA81-16910 to Brown University and by the donors of The Petroleum Research Fund, administered by the American Chemical Society, through grant PRF no. 15888-AC5. We gratefully acknowledge grants of computer time by the Scientific Computing Division at the National Center for Atmospheric Research that allowed use of their CRAY-1 computers on which these calculations were performed. NCAR is sponsored by NSF.

REFERENCES

AREF, H. & SIGGIA, E. D. 1980 Vortex dynamics of the two-dimensional turbulent shear layer. *J. Fluid Mech.* **100**, 705–737.

AREF, H. & TRYGGVASON, G. 1984*a* Vortex dynamics of passive and active interfaces. *Physica* **12D**, 59–70.

AREF, H. & TRYGGVASON, G. 1984*b* Interface dynamics by the vortex-in-cell method. *Presented at 16th Intl Congr. Theoretical and Applied Mechanics, Lyngby, Denmark.* (unpublished).

DE JOSSELIN DE JONG 1960 Singularity distributions for the analysis of multiple-fluid flow through porous media. *J. Geophys. Res.* **65**, 3739–3758.

MCLEAN, J. W. & SAFFMAN, P. G. 1981 The effect of surface-tension on the shape of fingers in a Hele-Shaw cell. *J. Fluid Mech.* **102**, 455–469.

PARK, C.-W., GORELL, S. & HOMSY, G. M. 1984 Two-phase displacement in Hele-Shaw cells: experiments on viscously driven instabilities. *J. Fluid Mech.* **141**, 257–287. Corrigendum: *J. Fluid Mech.* **144**, 468–469.

PARK, C.-W. & HOMSY, G. M. 1984 Two-phase displacement in Hele-Shaw cells: theory. *J. Fluid Mech.* **139**, 291–308.

PITTS, E. 1980 Penetration of fluid into a Hele-Shaw cell: the Saffman–Taylor experiment. *J. Fluid Mech.* **97**, 53–64.

SAFFMAN, P. G. 1959 Exact solutions for the growth of fingers from a flat interface between two fluids in a porous medium or Hele-Shaw cell. *Q. J. Mech. Appl. Maths* **12**, 146–150.

SAFFMAN, P. G. & TAYLOR, G. I. 1958 The penetration of a fluid into a porous medium or Hele-Shaw cell containing a more viscous liquid. *Proc. R. Soc. Lond.* A **245**, 312–329.

TAYLOR, G. I. & SAFFMAN, P. G. 1958 Cavity flow of viscous liquids in narrow spaces. In *Proc. 2nd Symp. on Naval Hydrodynamics.*

TAYLOR, G. I. & SAFFMAN, P. G. 1959 A note on the motion of bubbles in a Hele-Shaw cell and porous medium. *Q. J. Mech. Appl. Maths* **12**, 265–279.

TRYGGVASON, G. & AREF, H. 1983 Numerical experiments on Hele-Shaw flow with a sharp interface. *J. Fluid Mech.* **136**, 1–30.

VANDEN-BROECK, J.-M. 1983 Fingers in a Hele-Shaw cell with surface tension. *Phys. Fluids* **26**, 2033–34.

WOODING, R. A. 1969 Growth of fingers at an unstable diffusing interface in a porous medium or Hele-Shaw cell. *J. Fluid Mech.* **39**, 477–495.

WOODING, R. A. & MOREL-SEYTOUX, H. J. 1976 Multiphase fluid flow through porous media. *Ann. Rev. Fluid Mech.* **8**, 233–274.